Journal of Physics: Conference Series

Experimental and theoretical investigations of traditional solar still productivity in cold climatic

To cite this article: Naseer T. Alwan *et al* 2021 *J. Phys.: Conf. Ser.* **2119** 012096

IOP Publishing
doi:10.1088/1742-6596/2119/1/012096

Experimental and theoretical investigations of traditional solar still productivity in cold climatic

Naseer T. Alwan [1, 2], **S E Shcheklein**[1], **and O M Ali** [3]

[1]Ural Federal University, Yekaterinburg 620002, Russia
[2]Engineering Technical College of Kirkuk, Northern Technical University, 36001 Kirkuk, Iraq
[3]Renewable Energy Research Unit, Northern Technical University, 36001 Kirkuk, Iraq

E-mail: nassir.towfeek79@gmail.com

Abstract. Solar distillation is an important technology to get potable water from saltwater using clean and free solar energy. In the current study, an experimental and theoretical investigation of a single-slope traditional solar still was carried out, and the freshwater productivity and thermal efficiency were evaluated for four typical days (19/06, 17/07, 22/08, and 15/09) of 2019 by implementing temperature parameters in different points of the solar still, and the weather parameters such as solar radiation, and ambient air temperature. The study showed an acceptable agreement between the experimental and theoretical results with an average of 6.6% measured deviation of the experimental data. It was noticed that the highest values of productivity were recorded on July 17, 2019.

1. Introduction

A small solar distillation system can be a practical and economical solution. For the current and future demand for potable water, with the availability of water resources and a large amount of solar radiation in these remote areas, it is necessary to examine the factors affecting the performance of the solar stills and try to improve them and find ways to increase their productivity [1,2]. This process removes impurities and bacteria. Finally, clean water is obtained. The yield of solar stills depends mainly on weather conditions, and their design [3,4]. There are different designs for solar stills, the most common of which are single and double slope, the type is chosen depending on the design and operational requirements. Garg and Mann [5] carried out experimental investigation to know the impact of design parameters on the productivity of single and double slope solar distillers according to dry weather regions in India. It is concluded that the single-sloped solar still receives a higher amount of solar radiation in both stations at high and low latitudes as compared to their counterpart from double-slope solar distillation. Several experimental and theoretical investigations have been conducted on the single-slope solar still to test its performance. Saeed Nazari [6] carried out a theoretical and experimental investigation on improving the productivity of solar distiller with a single slope by adding copper oxide (Cu2O) nanoparticles to the basin water and providing the system with a condensation duct made of thermoelectric cells. The study showed that the condensation duct enhanced the productivity by 38.5%, and by about 82.4% when adding 0.08% of Cu2O nanoparticles in the basin water. The cost of producing one liter of distilled water was $ 0.021. Another study [7,8] was conducted to show the effect of the depth of basin water on the heat transfer coefficient and the performance of solar distillers with a single slope. The study showed that by decreasing the depth of water from 3 cm to 1 cm, the productivity increased by 52% with increasing internal coefficient of heat transfer. The highest coefficient of heat transfer was around 1:00 pm, with a water depth of (1 cm) of about 33.37 $W/m^2 \cdot K$, and the best cost to produce one liter of distilled water was \$ 0.033 at a depth of (1 cm). Naseer et al. [9] conducted an investigational study to show the effectiveness of using paraffin wax in solar stills. The paraffin was distributed in square cells to ensure uniform distribution of heat transfer to and from the paraffin wax. The results showed that paraffin wax cells augmented productivity by about 32%. Various works conducted investigations on the performance of traditional solar still in hot areas, but none of them examines the performance in cold regions such as the Russian Federation. Therefore, this study aims to verify the performance of traditional single-slope solar distiller experimentally and theoretically for four months (from June to September of 2019). A mathematical model has been built using the finite difference method and Fortran 90 programming language to predict the productivity and thermal performance of the traditional solar still (TSS) under different conditions.

2. Experimental setup

The traditional solar still consisted of a waterproof wooden frame, a plexiglass cover, a metal water basin of galvanized iron, painted pale black. The dimensions of the traditional solar still were mentioned in detail by Naseer T. Alwan et.al [10–13]. The rubber silicone was used for fixings. The surface area of the distiller was 0.5 m^2. Figure (1) illustrates the schematic diagram of the traditional solar still under study. The experimental study was conducted from June to September of 2019, with four typical clear days: 19.6.2019, 17.7.2019, 22.8.2019, and 15.9.2019.

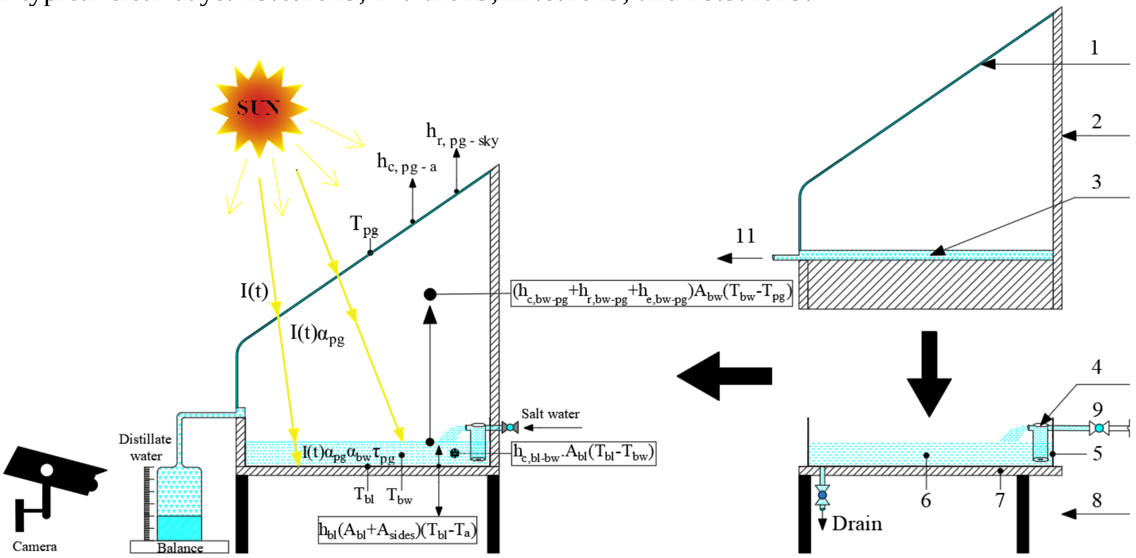

Figure 1. Schematic diagram of manufacturing stages of traditional solar still (TSS); 1. Plexiglass cover; 2. MDF wooden board; 3. U - aluminium channel; 4. Mechanical floater; 5. Basin; 6. Basin water; 7. Base; 8. Metal legs; 9. Globe valve; 10. Graduated cylinder; 11. Distillate water [18].

3. Numerical method

A theoretical analysis included the energy balance of the different components of the solar distiller by the Fortran 90 program. Figure 1 shows the different energies in the solar distiller that affected productivity directly. To simplify the mathematical analysis, the following has been assumed:
1) No leakage of air and vapor in the solar distiller. 2) Dry air and steam are treated as ideal gases. 3) Neglecting the dust and dirt on the Plexiglass cover. 4) There is temperature uniformity along with the Plexiglass cover (negligible heat absorbed by it) [9].

The energy balance equations for traditional solar still included the following components: basin liner, basin water, and a plexiglass cover. As it is shown in figure (1).

Basin water liner (bl) [8,9]**:**

$$I(t) \cdot A_{bl} \cdot \alpha_{bl} \cdot \tau_{Pg} \cdot \tau_{bw} = m_{bl} \cdot CP_{bl} \cdot \frac{dT_b}{dt} + h_{c,bl-bw} \cdot A_{bl} \cdot (T_{bl} - T_{bw}) + h_{bl} \cdot (A_{bl} + A_{sides}) \cdot (T_{bl} - T_a) \quad (1)$$

Where $I(t)$ is the solar radiation intensity (W/m^2), α_b is the absorptivity of the basin plate, $\alpha_{bl}\ and\ \tau_{bw}$ the transmittance of plexiglass cover and basin water, m_b is the basin plate mass (Kg), Cp_b is the specific heat of the basin plate $(J/kg.K)$, $h_{c,bl-bw}$ is the coefficient of heat transfer by convection from basin plate to water $(W/m^2.k)$ [8], A_{bl} is the basin surface area (m^2), T_{bl} is the basin liner temperature (°C), T_{bw} is the basin water temperature (°C),

$$h_{c,bl-bw} = 0.2\left(\frac{K_{bw}}{L_{bl}}\right) \cdot {R_a}^{0.26} \quad (2)$$

K_{bw} is the basin water thermal conductivity $(W/m.K)$, L_b is the characteristic length, and R_a represent the Rayleigh number [14]:

$$R_a = \frac{g \cdot \beta_{bw} \cdot {L_{bl}}^3}{\upsilon_{bw} \cdot \alpha_{bw}} [(T_{bw} - T_{Pg}) + \frac{(P_{bw} - P_{Pg})(T_{bw} + 273.15)}{2689 \cdot 10^2 - P_{bw}}) \quad (3)$$

g is the gravitational acceleration (9.81 m/s^2), υ_w is the kinematic viscosity of water (m^2/s), α_w is thermal diffusivity of water, β_{bw} is the thermal expansion coefficient of basin water according to [14]: $\beta_{bw} = 2/(T_{bw} - T_{bl})$, P_{bw} and P_{Pg} are Partial pressure of vapor at basin water and Plexiglass cover respectively, given as in [14], h_{bl} is the coefficient of heat transfer from the basin liner to ambient air $(W/m^2.k)$ which is obtained as in [15]:

$$h_{bl} = [\frac{L_i}{K_i} + \frac{1}{h_{t,bl-a}}]^{-1}, \quad (4)$$

Where L_i is the insulation thickness (cm) and K_i represents the thermal conductivity of the insulation $(W/m.k)$, $h_{t,bl-a}$ is the convection and radiation heat transfer coefficients from basin liner to the ambient air, $(W/m^2.k)$ is expressed as in [15]:

$$h_{t,bl-a} = 5.7 + 3.8 \cdot V_a, \quad (5)$$

Where V_a is the ambient air velocity (m/s), T_a is the ambient air temperature (°C), A_{sides} is the side surfaces area of the basin (m^2).

Basin water (bw) [8,9]**:**

$$I(t) \cdot A_{bw} \cdot \alpha_{bw} \cdot \tau_{Pg} + h_{c,bl-bw} \cdot A_{bw} \cdot (T_{bl} - T_{bw}) = m_{bw} \cdot CP_{bw} \left(\frac{dt_{bw}}{dt}\right) + (h_{c,bw-Pg} + h_{r,bw-Pg} + h_{e,bw-Pg}) \cdot A_{bw} \cdot (T_{bw} - T_{Pg}) \quad (6)$$

Where T_{Pg} is the temperature of the plexiglass cover (°C), m_{bw} is the basin water mass (Kg), CP_{bw} is the specific heat of the basin water $(J/kg.K)$, $h_{c,bw-Pg}$ is the coefficient of heat transfer by convection from water to the plexiglass cover $(W/m^2.k)$,

$$h_{c,bw-Pg} = 0.884 \cdot [(T_{bw} - T_{Pg}) + \frac{(P_{bw} - P_{Pg})(Tb_w + 273.15)}{(268900 - P_{bw})}]^{0.333}, \quad (7)$$

$h_{e,bw-Pg}$ is the coefficient of heat transfer by evaporation from water to the Plexiglass cover $(W/m^2.k)$ [16],

$$h_{e,bw-Pg} = 16.276 \cdot 10^{-3}\, h_{c,bw-Pg} \cdot \frac{(P_{bw} - P_{Pg})}{(T_{bw} - T_{Pg})} \quad (8)$$

$h_{r,bw-Pg}$ is the radiation heat transfer coefficient from water to the Plexiglass cover $(W/m^2.k)$ [16],

$$h_{r,bw-Pg} = \left(\frac{1}{\varepsilon_{bw}} + \frac{1}{\varepsilon_{Pg}} - 1\right)^{-1} \cdot \sigma \left[(T_{bw} + 273.15)^2 - \left(T_{Pg} + 273.15\right)^2\right] \cdot \left[T_{bw} + T_{Pg} + 546\right] \quad (9)$$

σ is Stefan Boltzmann constant, ε_g and ε_w are the plexiglass cover and the water-effective emissivity.

Plexiglass cover (Pg) [8,9]:

$$I(t)\cdot\ \alpha_{Pg}\cdot A_{Pg}+\left(h_{c,bw-Pg}+h_{r,bw-Pg}+h_{e,bw-Pg}\right)\cdot\left(T_{bw}-T_{Pg}\right)=m_{pg}\cdot Cp_{Pg}\cdot\frac{dT_{pg}}{dt}+$$
$$=\left(h_{c,Pg-a}+h_{r,Pg-sky}\right)\cdot\left(T_{Pg}-T_{a}\right) \qquad (10)$$

Where: A_{Pg} is the plexiglass cover surface area (m^2), $h_{c,Pg-a}$ is the convection heat transfer coefficient from plexiglass cover to the ambient air ($W/m^2.k$), [17], where $h_{c,Pg-a}=2.8+3V_a\ if\ V_a\leq 5\,m/s,$ or $h_{c,Pg-a}=5.7+2.8V_a\ \ if\ V_a>5\,m/s,$ $h_{r,pg-sky}$ is the coefficient of heat transfer by radiation from the outside surface Plexiglass cover for the exchange of radiation with the sky at T_{sky} ($W/m^2.k$),

$$h_{r,Pg-sky}=\varepsilon_{Pg}\cdot\sigma\left[\left(T_{sky}+273.15\right)^2-\left(T_{Pg}+273.15\right)^2\right]\left[T_{sky}+T_{Pg}+546\right] \qquad (11)$$

Hourly productivity of distilled water:

The yield output per hour in $L/m^2.hr$ hours is the heat transfer coefficient by evaporation ($h_{e,w-g}$) per surface area, multiplied by the temperatures difference between the water and the plexiglass cover $\left(T_{bw}-T_{Pg}\right)$, the results divided by mean latent heat h_{fg} in J / Kg [21]:

$$\dot{m}_w=\frac{h_{e,w-g}\cdot A_{bw}\cdot\left(T_{bw}-T_{pg}\right)}{h_{fg}} \qquad (12)$$

$$h_{fg}=1000*\left(2501.9-2.40706*T_{bw}+1.192217*10^{-3}*T_{bw}^2-1.5863\cdot 10^{-5}\cdot T_{bw}^3\right) \qquad (13)$$

Hourly thermal efficiency of the traditional solar still:

The hourly thermal efficiency (η_{hc}) of the traditional solar still was calculated by multiplying the hourly cumulative of distillate water ($\dot{m}_w$) by the average latent heat (h_{fg}), then the results were divided by the hourly solar radiation $I(t)$ over the whole area (0.5 m^2) and period ($3600\ s$):

$$\eta_{hc}=\frac{\dot{m}_w\cdot h_{fg}}{A_{bw}\cdot I(t)\cdot 3600}100\%$$

(14)

Numerical analysis of traditional solar water still requires initial boundary conditions for various parameters, such as basin water temperatures T_{bl}, basin water temperature T_{bw}, plexiglass cover temperature T_{Pg}. Also, this analysis required initial weather parameters such as ambient air temperature T_a^0 and wind speed V_a^0. The various parameters were expressed at the start of the running program at time equal to zero, which includes T_{Pg}^0, T_{bl}^0, and T_{bw}^0. Then the energy balance equations were applied to calculate the temperature values of the different parameters in the next step. The theoretical analysis in the current work was performed using the Fortran 90 (programming language) to estimate the yield of distillate water and traditional solar still efficiency, and the time step was 0.5 sec.

4. Results and discussion

To verify the validity of the theoretical model, a comparison of its results with the experimental data was carried out for 12 hours (08:00 am-8:00 pm). In the theoretical model, the weather and operational parameters were used to run the program. Figures (2,3, and 4) show the theoretical and experimental results, which included the relationship between the different parameters (temperature and weather parameters, distillate water productivity, thermal efficiency) and hourly local time for four typical days for four different test months of 2019. The study showed an acceptable agreement between the experimental and theoretical results with an average of 6.6% measured deviation of the experimental data. Figure 2 (a, b, c, and d) shows the hourly change of the temperatures at different points of traditional solar still and weather parameters for four different test months of 2019. From this figure, it is noticed that the temperature parameters at different parts of the traditional solar distiller (T_{bl}, T_{bw}, and T_{Pg}) were directly affected by weather conditions. In the early hours of sunrise, the level of solar radiation was relatively low and increased with the progression of time, reaching its peak at midday at about 1:00 pm or 2:00 pm. After that, it gradually decreased until sunset. The basin liner and basin water temperatures were lower than the plexiglass temperature in the early morning hours (because the heat capacity of water is greater than that of the plexiglass). After 09:00 am, the basin liner and basin water temperatures began to increase and exceed the plexiglass temperature, reaching the highest values at midday (1:00 - 2:00 pm) at the highest received solar radiation, after 2:00 pm the temperature of the cover decreased with a decrease in the level of solar radiation, and the highest temperature values were on 17 July of 2019 because the weather conditions (solar radiation and ambient air temperature) are higher than in other months. The highest temperature values for the basin plate, water, and plexiglass cover were recorded in midday at 2:00; they were about (60.3 ℃, 57 ℃, and 47 ℃ for theoretical model) and (58.3 ℃, 56.1 ℃, and 46.1 ℃ for experimental data), while the values of solar radiation and ambient air temperature were about 828.7. W/m^2 and 32.2 ℃.

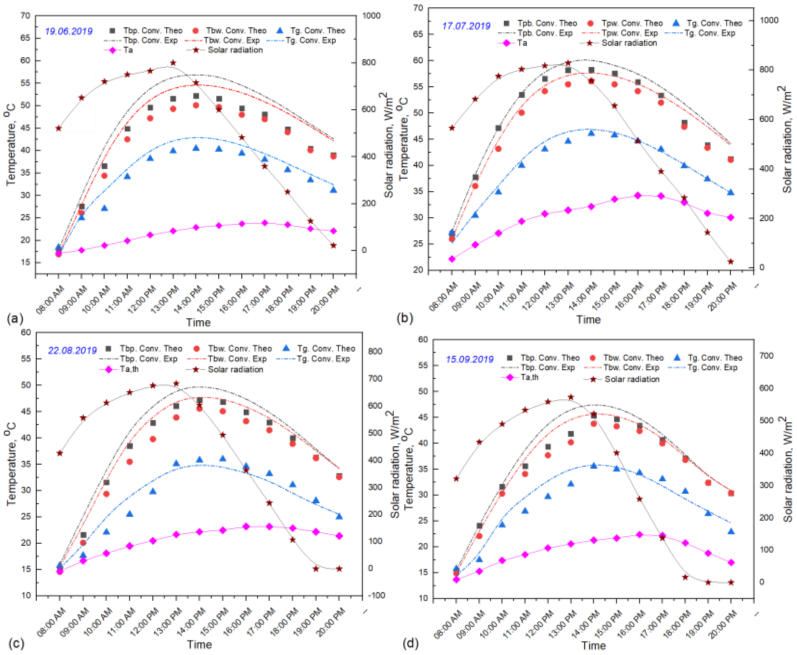

Figure 2. The hourly change of the temperatures at different points of conventional solar still and weather parameters for four different test months of 2019.

Figure (3) shows the cumulative productivity of traditional solar still for a typical four days of four different test months of 2019. The weather parameters (solar radiation, ambient air temperature) and water temperature can be taken as the most important factors that have a direct impact on the daily yield of the solar distiller under study. The highest productivity per hour was recorded on 17 July of 2019 throughout the day, as compared to the other typical days for the other test months, and the peak yield was after midday at 4:00 pm (350 $ml\ /m^2.hr$) because the basin water got enough latent heat to evaporate as well as a decrease in the Plexiglass cover temperature (due to the low ambient air temperature). Therefore, the highest cumulative yield of distilled water was 2800 $ml/m^2 \cdot hr$ on July 17, followed by (2600, 2200, and 1600) $ml/m^2 \cdot hr$ for other typical days (16 June, 22 August, and 15 September) of 2019 respectively, as shown in Figure 3 (a, b, c and d). Also, it can be noted from this figure that the results of the theoretical model gave an acceptable agreement with the experimental data on average deviation of 8.39%, due to the error generated when measuring and recording experimental data. To choose the best solar still design, the thermal efficiency must be evaluated. It is noticed from Figure 4 (a, b, c and d) that the thermal efficiency increased over time until it reached its highest value after 2:00 pm, as the solar radiation intensity decreased and the distillate water productivity increased (the potential energy of water evaporation increased). This is because the heat energy loss from the Plexiglass cover to the ambient air in this period promoted the condensation process (increased productivity). The average hourly thermal efficiency of traditional solar still for four typical days (19 June, 17 July, 22 August, and 15 September) of 2019 was about 48%, 42%, 50%, and 52%, respectively. However, when the relative humidity was relatively low, the intensity of the solar radiation was appropriate and the ambient air temperature was relatively high.

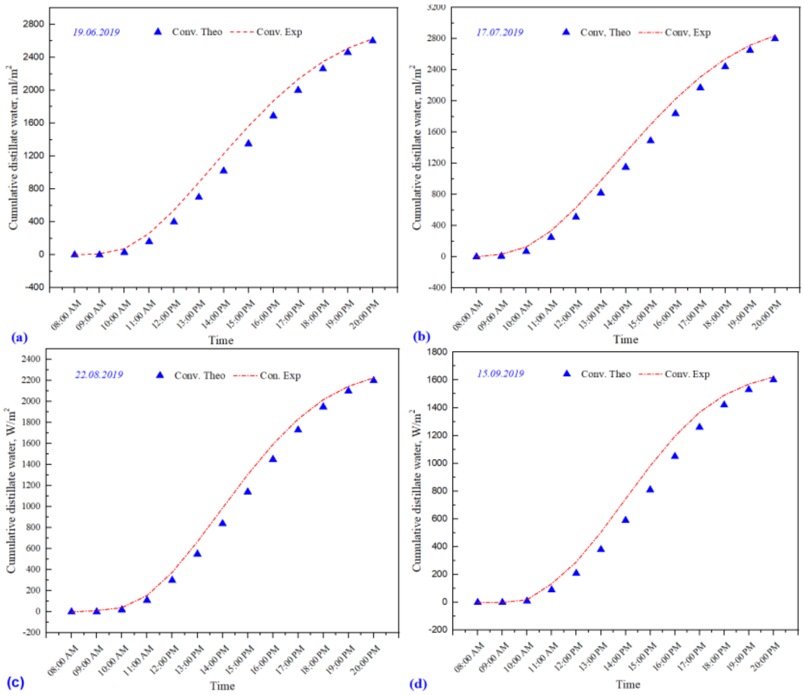

Figure 3. The hourly change of the cumulative distilled water for four different test months of 2019.

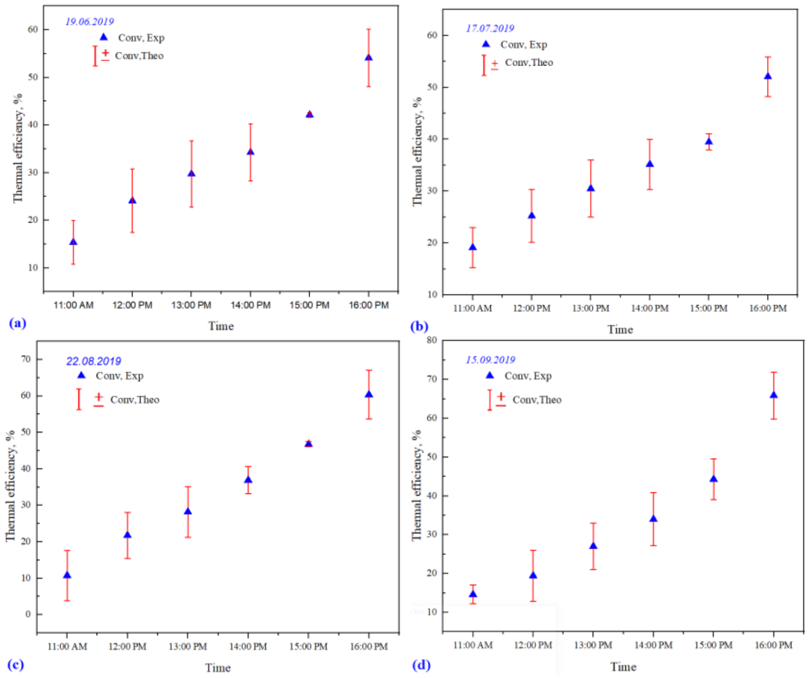

Figure 4. The hourly change of thermal efficiency for four typical days of 2019.

5. Conclusions

In this work, the following conclusions were obtained:

a) Weather parameters have a direct effect on the hourly yield of the solar still. The rate of productivity increases with the growth of the values of solar radiation and the decrease in the ambient air temperature, this is what characterizes the current work with the availability of these two important factors,

b) The maximum efficiency in the afternoon was recorded because the potential energy of water evaporation increased.

c) The optimum thermal efficiency of traditional solar still of about 72% was on 2 October of 2019, while the lowest thermal efficiency of about 52% was recorded on 17 July of 2019.

d) The proposed mathematical model gave good agreement with experimental results, this model can be used in the future to estimate the performance and productivity of solar stills, thus achieving an economic and time goal.

References

[1] Deceased J A D and Beckman W A 2013 *Solar Engineering of Thermal Processes*
[2] Foster R, Cota A and Group F 2010 *SOLAR ENERGY "Renewable Energy and the Environment"* (London New York: CRC Press) 337
[3] Alhayeka I and Badran O 2004 *Desalination* **169** 121–7
[4] Al-Hinai H, Al-Nassri M S and Jubran B A 2002 *Energy Convers. Manag.* **43** 1639–50
[5] Garg H P and Mann H S 1976 *Solar Energy* **18** (2) 159–163
[6] Nazari S, Safarzadeh H and Bahiraei M 2019 *Energy* **135** 729–44
[7] Alwan N T, Shcheklein S E and Ali O M 2020 *J. Phys. Conf. Ser.* **1706**
[8] Alwan N T, Shcheklein S and Ali O 2020 *Energy Sources, Part A Recover. Util. Environ. Eff.* 1–18
[9] Alwan N T, Shcheklein S E and Ali O M 2019 *Int. J. Energy Convers.* **7** 162–70
[10] Alwan N T, Shcheklein S E and Ali O M 2020 *AIP Conference Proceedings* **2290** 50023
[11] Naseer T A, Shcheklein S E and Ali O M 2020 *Appl. Sol. Energy* **56** 276–83
[12] Alwan N T, Shcheklein S E and Ali O M 2020 *IOP Conference Series: Materials Science and Engineering* **745**
[13] Alwan N T, Shcheklein S E and Ali O M 2020 *IOP Conference Series: Materials Science and Engineering* **791**
[14] Malaeb L, Aboughali K and Ayoub G M 2016 *Sol. Energy* **125** 360–72
[15] Medugu D W and Ndatuwong L 2009 *International Journal of Physical Sciences* **4** (11) 705-712
[16] Alwan N T, Shcheklein S E and Ali O M 2020 *Int. J. Des. Nat. Ecodynamics* **15** 57–64
[17] Sarhaddi F 2018 *Renew. Power Gener.* **12** 1336–44
[18] Alwan N T, Shcheklein S E E and Ali O M 2020 *Case Stud. Therm. Eng.* **19** 100614